Available online at www.sciencedirect.com

SciVerse ScienceDirect

Ceramics International 38 (2012) 1867–1872

CERAMICS INTERNATIONAL

www.elsevier.com/locate/ceramint

Oxygen permeation properties of BSCF5582 tubular membrane fabricated by the slip casting method

M.-B. Choi, D.-K. Lim, S.-Y. Jeon, H.-S. Kim, S.-J. Song *

Department of Materials Science and Engineering, Chonnam National University, 300 Yongbong-dong, Buk-gu, Gwangju 500-757, South Korea

Received 12 September 2011; received in revised form 3 October 2011; accepted 4 October 2011
Available online 8 October 2011

Abstract

BSCF5582 tubular oxygen separation membranes were prepared using the most cost effective slip casting techniques. The optimum slurry composition was identified and a dense, and crack free 60 mm long BSCF5582 tubular membrane being successfully prepared after the programmed sintering process. The effects of the feed flow rate and the sweeping flow rate on the oxygen permeation flux of the tubular BSCF5582 membrane were investigated. The oxygen permeation flux increased with an increase of the oxygen chemical potential gradient to a maximum of 42.5 cm^3/min in an O_2/N_2 condition at 1223 K for the 1.5 mm thick, 60 mm long BSCF tube, a value which corresponds to 1.42 cm^3/min cm^2. The ionic conductivity of the oxygen was successfully calculated in the dominant electron conducting regime. The ionic conductivity was found to increase with an increase of the temperature to 900 °C, indicating that it is a thermally activated process with an activation energy of 0.70 ± 0.1 eV in an air environment.

Keywords: A. Slip casting; E. Membranes; Oxygen

1. Introduction

A variety of ionic-electronic conducting perovskite oxide structures with an ABO_3-type molecular formula have been identified as promising materials for the separation of oxygen from a variety of oxygen containing gas mixtures [1–5]. Despite the excellent rate of oxygen diffusion and the fast surface exchange rate [6–9], Co-based perovksite membranes have not been successful as an oxygen separation membrane application due to their high thermal and chemical expansion properties [10,11], and their low chemical stability at a low oxygen partial pressure [12–14]. Recently, there have been many studies suggesting that cobalt based perovskite membranes are able to operate stably under light hydrocarbon conversion, oxygen separation above 10^{-8} atm and in water splitting conditions [15–17]. In particular BSCF5582 ($Ba_{0.5}Sr_{0.5}Co_{0.8}Fe_{0.2}O_{3-\delta}$) with a substitution of Sr with Ba, which has a larger ionic radius than Ba and the same valence state, has been identified as possessing good phase stability and an excellent oxygen permeability.

To increase the oxygen permeation flux through the BSCF5582 membranes as a result of an enlarged active membrane surface, tubular and planar type designs have been developed most frequently [18–20]. Compared to the planar type of membrane, the tubular design possesses obvious advantages for industrial applications, although much more difficult to attain, it not only offers much better stability during thermal cycling and avoids sealing problems but also has a larger reaction area to volume ratio than the planar type membrane. Generally there have been two methods explored for the fabrication of membranes in the form of dense tubular type membranes, one being the isostatic pressing method and the other the plastic extrusion method. The plastic extrusion method can prepare the membrane with a variety of shapes and sizes more easily. In addition, plastic extrusion techniques for fabricating the tubular membrane are more accepted as favorable methods for mass production, though the large batch quantity and the plastic extrusion equipment requirement results in high costs. Slip casting techniques, on the other hand, may offer additional advantages. Tubular membranes derived from the slip casting process exhibit good compositional homogeneity and can be prepared over a wide range of compositions in a relatively simple manner [21]. Furthermore,

* Corresponding author. Tel.: +82 62 530 1706; fax: +82 62 530 1699.
E-mail addresses: song@jnu.ac.kr, song@chonnam.ac.kr (S.J. Song).

0272-8842/$36.00
doi:10.1016/j.ceramint.2011.10.012

slip casting methods require less equipment and are thus less expensive than other techniques.

In this study, BSCF5582 tubular membranes were prepared using the most cost-effective slip casting techniques without further experimental setups. The effects of the feed flow rate and the sweeping flow rate on the oxygen permeation flux of the tubular BSCF5582 membrane was investigated. The oxygen permeation flux as a function of temperature and the oxygen partial pressure gradient was studied and the ionic conductivity of the oxygen was successfully calculated in the dominant electron conducting regime.

2. Experimental

Perovskite BSCF5582 powders were prepared using the conventional solid state reaction method. The starting materials, $SrCO_3$ (Aldrich, 99.99%), $BaCO_3$ (Aldrich, 99.99%), F_2O_3 (Aldrich, 99.9%) and Co_3O_4 (Aldrich, 99.9%) were weighed to make the stoichiometric proportions for BSCF5582. The powders were mixed and then ground in a ball mill with stabilized zirconia balls, then calcined in air for 10 h at 1223 K. The calcined oxide powders were then crushed and sieved to produce a size of <45 μm. As shown in Fig. 1, the X-ray diffraction spectra confirmed the attainment of a single phase, cubic BSCF (space group, *Pm-3m*) via the solid state reaction method.

The prepared BSCF powders were then dispersed into a mixture of ethanol and dispersant (Cerasperse 5468, ammonium salt of polycarboxylic acid), with the slurry then being ball milled for 24 h with stabilized zirconia balls. The deforming agent (SN-deformer 485, polyether), plasticizer (polyvinyl alcohol) and binder (PEG 400, polyethylene glycol) were subsequently introduced into this BSCF slurry. The slurry was then ball milled with the stabilized zirconia balls for another 24 h to break up the agglomerated powders and the BSCF slurry was then used to fabricate the tube using the slip casting method. When the well mixed BSCF5582 powder slurry is poured into a microporous mold, the suspension of the solvent is attracted into the pores of the mold as a result of the capillary suction pressure. The slip particles are therefore consolidated on the surface of the mold to form a particle or gel layer [22]. The cast BSCF green tube was further dried and the 10 cm-long BSCF tube was then sintered.

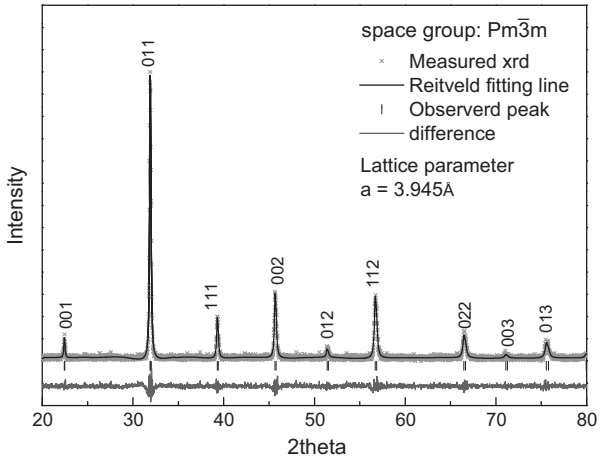

Fig. 1. XRD patterns of $Ba_{0.5}Sr_{0.5}Co_{0.8}Fe_{0.2}O_{3-\delta}$.

The top planar end surface of the sintered BSCF tubes was polished with 600-grit SiC paper and affixed to an alumina tube with a ceramic sealant (Aremco, #571), which formed a seal when the assembly was heated to 1233 K. The sweep side flow consisted of ultra-high purity He, while the feed gas flow consisted of a mixture of air and N_2. The sweep gas flow was controlled during the permeation measurements with a mass flow controller and the rate measured with a flow calibrator (Digital flowmeter, Optiflow 570). The oxygen content of the permeate stream was measured using a gas chromatograph (Agilent 6890N) with a TC detector. Any gas leakage through the pores in the sample or through an incomplete seal was detected by measuring the N_2 content of the permeate stream.

3. Results and discussion

In order to prepare a mixed, dense, conducting and oxygen separating BSCF5582 tube, the slip casting method was applied with a porous alumina mold being used. The capillary suction pressure was inversely correlated with the pore radius of the mold, indicating that a decrease in the porosity of the BSCF5582 green tube increased the casting rate [21]. Moreover, a well dispersed slip, which contains no agglomerates and is stabilized by steric repulsion, formed a fairly dense cast with better microstructural uniformity. The consolidation rate and thickness were determined via careful control of the volume fraction of the solids in the slurry and the casting time using a trial and error approach in this study. The optimum surfactant quantities in this work were identified and are shown in Table 1. The optimized BSCF5582 slurry was then applied to the alumina mold to form a green tube as shown in Fig. 2. The cast green BSCF tube was then further dried for 2 h in an air drying oven, after partial drying inside the mold for 24 h. The cast, 10 cm-long, BSCF tube was then sintered in air for 10 h at 1323 K to obtain a mechanically strong support with additional pre-heating in air for 4 h at 723 K. The shrinkage during sintering was around 27%, with the diameter decreasing from 30 mm to 22 mm. Surface images of the BSCF sintered tube, prepared using the proposed slip casting method, are shown in Fig. 3a. The microscopic SEM surface images show a structure with well necked grains. The cross sectional image in Fig. 3b

Table 1
Optimum slurry composition for $Ba_{0.5}Sr_{0.5}Co_{0.8}Fe_{0.2}O_{3-\delta}$ tube fabrication using the slip casting method.

Components	Dosage
BSCF5582	100 g
Ethanol	30 g
HS-dispersant 5801 (deflocculant)	2 g
Ball milling for 4 h	
SN-Defoamer 485 (defoamer)	1 g
PVB (10% sol)	1.5 g
Ball milling for 2 h	

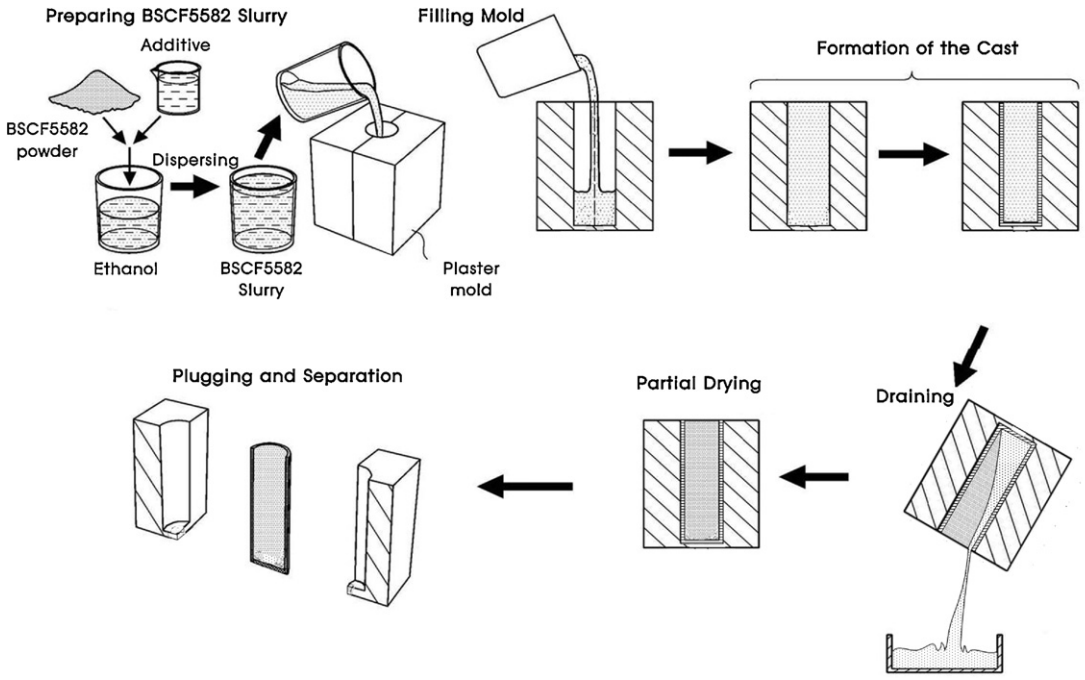

Fig. 2. Schematic diagram for the fabrication of $Ba_{0.5}Sr_{0.5}Co_{0.8}Fe_{0.2}O_{3-\delta}$ tube using the slip casting method.

also shows the successful fabrication of a dense BSCF oxygen separation membrane, with the densities of the resultant disks being 96% of the theoretical values. The BSCF5582 tube used for the oxygen permeation measurements were cut out of the sintered tube to 60 mm long by 1.5 mm thick and a 22 mm outer diameter as shown in Fig. 4.

The influence of the gas flow rate on the feed and sweep sides on the oxygen permeability of the BSCF tube is shown in Fig. 5. The oxygen concentration distribution profile along the 60 mm long tube was expected as the linear gas flow direction being parallel to the tube may cause inhomogeneity in the flowing gas composition, resulting in a varying oxygen permeation rate. Over the flow rate range investigated, 100–200 sccm on the feed side, with a fixed 100 sccm helium sweep flow rate, the oxygen permeation flux monotonically increased with an increase of the flow rate to a maximum of 8 $cm^3/min\ cm^2$ and reached a saturation point at around 200 sccm and 1173 K as shown in Fig. 5a. This suggests that the surface diffusion or the surface exchange rate of the oxygen on the membrane surface inside the tube may not be the limiting step for oxygen permeation when the air flow rate is higher than 200 sccm. The effect of the helium flow rate in the outside of the tube on the total oxygen permeation flux was also investigated. With a fixed feed flow rate and an increasing of the helium sweep flow rate from 100 to 200 sccm, the oxygen permeation rate increased and saturated at around 200 sccm, as shown in Fig. 5b. The increase in the oxygen permeation flux may be understood by the fast removal of permeated oxygen from the outside of the tubular membrane, resulting in a constant oxygen partial pressure gradient across the membranes. Therefore, a gas flow rate of 200 sccm was maintained on both sides of the tube for further oxygen permeation measurements.

The influence of the applied oxygen chemical potential gradient on the oxygen permeability of BSCF5582 over a range of temperatures is shown in Fig. 6. The oxygen permeation flux increased with an increase of the oxygen chemical potential

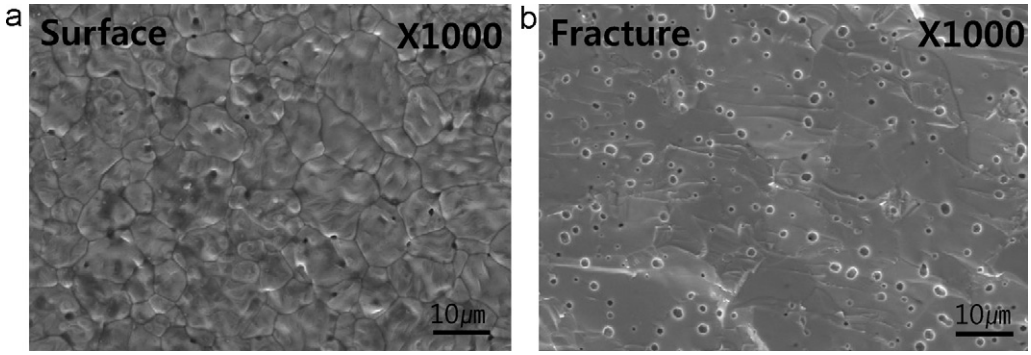

Fig. 3. SEM (scattering electron micrography) images of (a) the outer surface and (b) the fracture surface of the sintered $Ba_{0.5}Sr_{0.5}Co_{0.8}Fe_{0.2}O_{3-\delta}$ tube from the drain casting method.

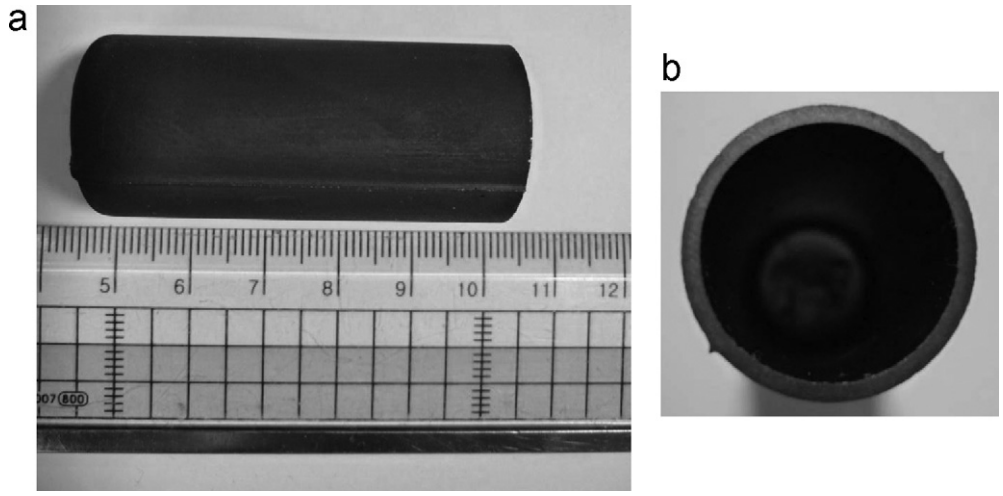

Fig. 4. Macroscopic image of (a) the as sintered and (b) the top view of the $Ba_{0.5}Sr_{0.5}Co_{0.8}Fe_{0.2}O_{3-\delta}$ tube.

gradient to a maximum of 42.5 cm^3/min in O_2/N_2 conditions at 1223 K for the 1.5 mm-thick BSCF5582 specimen. This corresponds to a rate of 1.42 cm^3/min cm^2 which is somewhat lower than the reported values of other authors from a disk type specimen [23]. The most plausible reason for this underestimation of the oxygen permeation flux may be ascribed to the varying oxygen chemical potential gradient along the BSCF5582 tube. This is not only due to the fact that the parallel feed gas flow may lead to a uniform oxygen concentration distribution profile, but also because the permeated oxygen may not sweep out from the tube surface uniformly. In either case, this may provide a position dependent oxygen potential gradient along the tube so that gas flow in the normal direction to the tube surface will be necessary with a further increase of the gas flow rate to optimize the process for the tube type oxygen separation membrane.

The ionic conductivity of the BSCF was also determined from the oxygen permeation measurements. As the electronic conductivity is expected to be several orders of magnitude greater than the oxygen ion conductivity, the oxygen permeation measurements can be applied to determine the oxygen ion conductivity. If bulk diffusion is assumed, the oxygen permeation flux across an oxide membrane can be derived from the chemical diffusion as stated by Wagner [24]:

$$J_{O_2} = -\frac{RT}{16LF^2}\int_{\ln P'_{O_2}}^{\ln P''_{O_2}} \frac{\sigma_{el}\sigma_{ion}}{\sigma_{el}+\sigma_{ion}}\, d\ln P_{O_2} \quad (1)$$

where σ_{el} and σ_{ion} are the electronic and ionic conductivities respectively, F is the Faraday constant and $d\ln P_{O_2}$ is the oxygen chemical potential gradient across an oxide membrane. The high total electrical conductivity of the BSCF5582 is generally attributed to the hopping of small p-type polarons, associated with the charge disproportionation of the B-site cations [25,26]. As the electronic transference number is believed to be dominant ($\sigma_{ion} \ll \sigma_{el}$), the ionic conductivity may be obtained by differentiation of Eq. (1) to give the following equation:

$$\sigma_{ion} = \frac{16F^2L}{RT}\left[\frac{\partial J_{O_2}}{\partial \ln P'_{O_2}}\right]_{P''_{O_2}} \quad (2)$$

The data set for different oxygen partial pressure gradients was obtained while the oxygen partial pressure on the reference side was kept constant. In this calculation, the mean slope at a

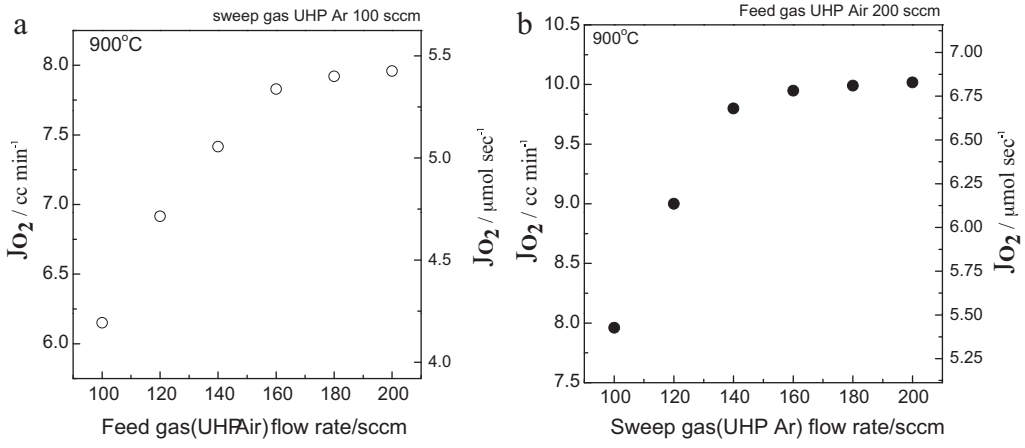

Fig. 5. (a) Sweep-side and (b) feed-side flow rate dependence of the oxygen permeation flux through the $Ba_{0.5}Sr_{0.5}Co_{0.8}Fe_{0.2}O_{3-\delta}$ tube at 1173 K.

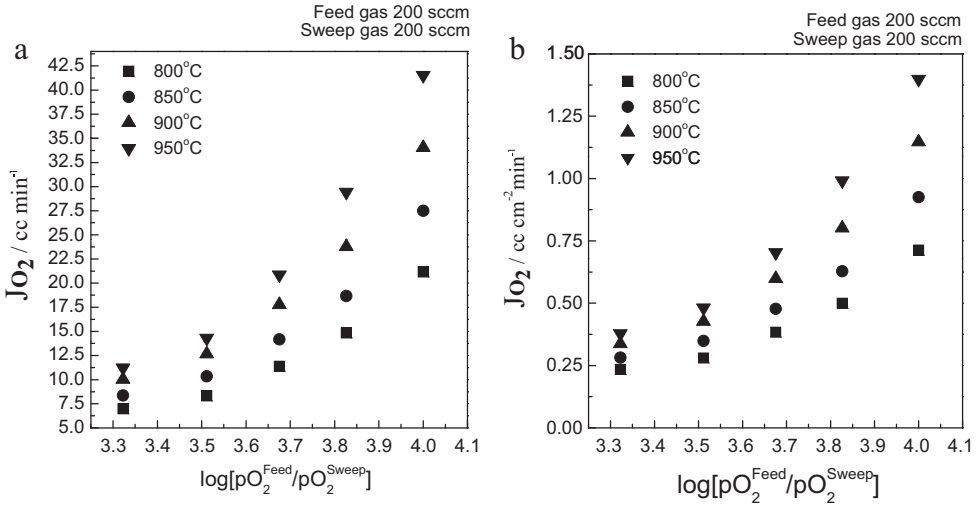

Fig. 6. (a) Total oxygen permeation flux and (b) normalized oxygen permeation flux of the $Ba_{0.5}Sr_{0.5}Co_{0.8}Fe_{0.2}O_{3-\delta}$ tube with a 200 sccm feed and sweep flow rate at 1173 K.

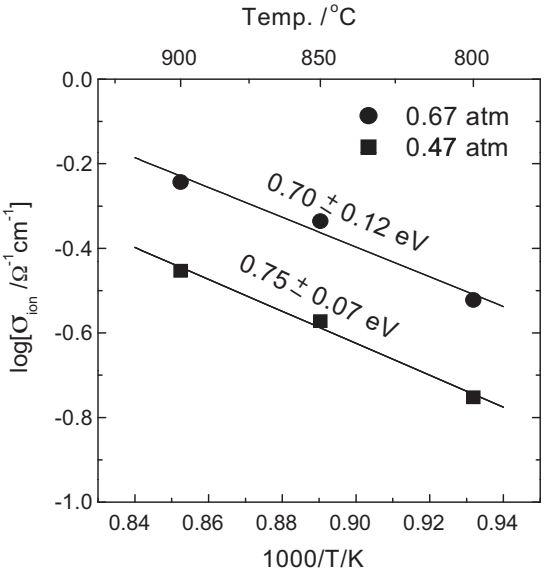

Fig. 7. Oxygen ion conductivity of $Ba_{0.5}Sr_{0.5}Co_{0.8}Fe_{0.2}O_{3-\delta}$ calculated from the oxygen permeation flux.

given value of P'_{O_2} was determined using the datum at P'_{O_2} and interpolating between its nearest neighbors. The calculated ionic conductivity at various oxygen partial pressures as a function of temperature is shown in Fig. 7. The oxygen ion conductivity was around 0.21 S/cm under air conditions and was found to decrease with a decreasing oxygen partial pressure at 900 °C, suggesting p-type conduction properties. The ionic conductivity increased with an increase of the temperature up to 900 °C, indicating that it is a thermally activated process with an activation energy of 0.70 ± 0.1 eV under air conditions. These findings show good agreement with the values found in the literature within the experimental uncertainty level [14,23,27].

4. Conclusion

In this work, BSCF5582 tubular membranes were prepared using the most cost effective slip casting techniques available without further experimental setups. The optimum slurry composition has been identified and a dense, crack free, 60 mm long BSCF5582 tubular membrane was successfully prepared after a programmed sintering process. The effects of the feed flow rate and the sweeping flow rate on the oxygen permeation flux of the tubular BSCF5582 membrane were investigated. The oxygen permeation flux increased with an increase of the oxygen chemical potential gradient to a maximum of 42.5 cm^3/min under O_2/N_2 conditions at 1223 K for the 1.5 mm-thick, 60 mm-long BSCF5582 tube, corresponding to a rate of 1.42 cm^3/min cm^2. A lower value of the permeation flux than the values reported from a disk type specimen were ascribed to the varying oxygen chemical potential gradient along the BSCF5582 tube. The oxygen ionic conductivity was successfully calculated in the dominant electron conducting regime. The ionic conductivity increased with an increase of the temperature up to 900 °C, indicating that it is a thermally activated process with an activation energy of 0.70 ± 0.1 eV under air conditions. This agrees well with the values found in the literature within the experimental uncertainty level.

Acknowledgements

The following are results of a study on the "Human Resource Development Center for Economic Region Leading Industry" Project, supported by the Ministry of Education, Science & Tehnology (MEST) and the National Research Foundation of Korea (NRF).

References

[1] Z. Shao, G. Xiong, J. Tong, H. Dong, W. Yang, Ba effect in doped $Sr(Co_{0.8}Fe_{0.2})O_{3-\delta}$ on the phase structure and oxygen permeation properties of the dense ceramic membranes, Sep. Purif. Technol. 25 (2001) 419–429.
[2] K. Zhang, Y. Yang, D. Ponnusamy, A. Jacobson, K. Salama, Effect of microstructure on oxygen permeation in $SrCo_{0.8}Fe_{0.2}O_{3-\delta}$, J. Mater. Sci. 34 (1999) 1367–1372.
[3] J.B. Smith, T. Norby, On the steady state oxygen permeation through $La_2NiO_{4+\delta}$ membranes, J. Electrochem. Soc. 153 (2) (2006) A233–A238.

[4] J.A. Lane, S.J. Benson, D. Waller, J.A. Kilner, Oxygen transport in $La_{0.6}Sr_{0.4}Co_{0.2}Fe_{0.8}O_{3-\delta}$, Solid State Ionics 121 (1999) 201–208.
[5] V.V. Kharton, A.A. Yaremchenko, A.V. Kovalevsky, A.P. Viskup, E.N. Naumovich, P.F. Kerko, Perovskite-type oxides for high-temperature oxygen separation membranes, J. Membr. Sci. 163 (1999) 307–317.
[6] S. McIntonsh, J.F. Vente, W.G. Haije, D.H.A. Blank, H.J.M. Bouwmeester, Structure and oxygen stoichiometry of $SrCo_{0.8}Fe_{0.2}O_{3-\delta}$ and $Ba_{0.5}Sr_{0.5}Co_{0.8}Fe_{0.2}O_{3-\delta}$, Solid State Ionics 177 (2006) 1737–1742.
[7] H. Wang, C. Tablet, A. Feldhoff, J. Caro, Investigation of phase structure, sintering, and permeability of perovskite-type $Ba_{0.5}Sr_{0.5}Co_{0.8}Fe_{0.2}O_{3-\delta}$ membranes, J. Membr. Sci. 262 (2005) 20–26.
[8] S. Li, Z. Lu, X. Huang, B. Wei, W. Su, Thermal, electrical, and electrochemical properties of lanthanum-doped $Ba_{0.5}Sr_{0.5}Co_{0.8}Fe_{0.2}O_{3-\delta}$, J. Phys. Chem. Solids 68 (2007) 1707–1712.
[9] D. Chen, Z. Shao, Surface exchange and bulk diffusion properties of $Ba_{0.5}Sr_{0.5}Co_{0.8}Fe_{0.2}O_{3-\delta}$ mixed conductor, Int. J. Hydrogen Energy 36 (2011) 6948–6956.
[10] S. McIntosh, J.V. Vente, W. Wim, D.H.A. Blank, H.J.M. Bouwmeester, Oxygen stoichiometry and chemical expansion of $Ba_{0.5}Sr_{0.5}Co_{0.8}Fe_{0.2}O_{3-\delta}$ measured by in situ neutron diffraction, Chem. Mater. 18 (2006) 2187–2193.
[11] R. Kriegel, R. Kircheisen, J. Topfer, Oxygen stoichiometry and expansion behavior of $Ba_{0.5}Sr_{0.5}Co_{0.8}Fe_{0.2}O_{3-\delta}$, Solid State Ionics 181 (2010) 64–70.
[12] J. Ovenstone, J.-I. Jung, J.S. White, D.D. Edwards, S.T. Misture, Phase stability of BSCF in low oxygen partial pressures, J. Solid State Chem. 181 (2008) 576–586.
[13] Z. Shao, W. Yang, Y. Cong, H. Dong, J. Tong, G. Xiong, Investigation of the permeation behavior and stability of a $Ba_{0.5}Sr_{0.5}Co_{0.8}Fe_{0.2}O_{3-\delta}$ oxygen membrane, J. Membr. Sci. 172 (2000) 177–188.
[14] E. Bucher, A. Egger, P. Ried, W. Sitte, P. Holtappels, Oxygen nonstoichiometry and exchange kinetics of $Ba_{0.5}Sr_{0.5}Co_{0.8}Fe_{0.2}O_{3-\delta}$, Solid State Ionics 179 (2008) 1032–1035.
[15] A. Leo, S. Liu, J.C. Diniz da Costa, Production of pure oxygen from BSCF hollow fiber membranes using steam sweep, Sep. Purif. Technol. 78 (2011) 220–227.
[16] H. Wang, Y. Cong, W. Yang, Investigation on the partial oxidation of methane to syngas in a tubular $Ba_{0.5}Sr_{0.5}Co_{0.8}Fe_{0.2}O_{3-\delta}$ membrane reactor, Catal. Today 82 (2003) 157–166.
[17] S. Engels, F. Beggel, M. Modigell, H. Stadler, Simulation of a membrane unit for oxyfuel power plants under consideration of realistic BSCF membrane properties, J. Membr. Sci. 359 (2010) 93–101.
[18] H. Wang, R. Wang, D.T. Liang, W. Yang, Experimental and modeling studies on $Ba_{0.5}Sr_{0.5}Co_{0.8}Fe_{0.2}O_{3-\delta}$ (BSCF) tubular membranes for air separation, J. Membr. Sci. 243 (2004) 405–415.
[19] S. Li, H. Qi, N. Xu, J. Shi, Tubular dense perovskite type membranes. Preparation, sealing and oxygen permeation properties, Ind. Eng. Chem. Res. 38 (1999) 5028–5033.
[20] H. Wang, Y. Cong, W. Yang, Oxygen permeation study in a tubular $Ba_{0.5}Sr_{0.5}Co_{0.8}Fe_{0.2}O_{3-\delta}$ oxygen permeable membrane, J. Membr. Sci. 210 (2002) 259–271.
[21] M.-B. Choi, S.-J. Song, T.-W. Lee, H.-I. Yoo, U.-D. Lee, B.-R. Bang, Preparation of asymmetric tubular oxygen separation membrane with oxygen permeable $Pr_2Ni_{0.75}Cu_{0.25}Ga_{0.05}O_{4+\delta}$, Int. J. Appl. Ceram. Technol. 8 (4) (2011) 800–808.
[22] Kang Li, Mixed conducting ceramic membranes for oxygen separation, in: Ceramic Membranes for Separation and Reaction, John Wiley & Sons, Inc., 2007, pp. 169–215.
[23] W.-K. Hong, G.-M. Choi, Oxygen permeation of BSCF membrane with varying thickness and surface coating, J. Membr. Sci. 346 (2010) 353–360.
[24] H.J.M. Bouwmeester, A.J. Burggraaf, Dense ceramic membranes for oxygen separation, in: P.J. Gelling, H.J.M. Bouwmeester (Eds.), The CRC Handbook of Solid State Electrochemistry, CRC Press, New York, 1997 pp. 481–554.
[25] J.-I. Jung, S.T. Misture, D.D. Edwards, Oxygen stoichiometry, electrical conductivity, and thermopower measurements of BSCF ($Ba_{0.5}Sr_{0.5}Co_{0.8}Fe_{0.2}O_{3-\delta}$, $0 \leq x \leq 0.8$) in air, Solid State Ionics 181 (2010) 1287–1293.
[26] Z. Shao, S.M. Haile, A high-performance cathode for the next generation of solid-oxide fuel cells, Nature 43 (2004) 170–173.
[27] L. Wang, R. Merkle, J. Maier, T. Acartork, U. Starke, Oxygen tracer diffusion in dense $Ba_{0.5}Sr_{0.5}Co_{0.8}Fe_{0.2}O_{3-\delta}$ films, Appl. Phys. Lett. 94 (2009) 071908.